Chromatin condensation of *Xist* genomic loci during oogenesis in mice

Atsushi Fukuda[1], Atsushi Mitani[1,2], Toshiyuki Miyashita[2], Akihiro Umezawa[1] and Hidenori Akutsu[1,3]*

[1]Center for Regenerative Medicine, National Research Institute for Child Health and Development, 2-10-1 Okura, Setagaya, Tokyo 157-8535, Japan

[2]Department of Molecular Genetics, Kitasato University Graduate School of Medical Sciences, 1-15-1 Kitasato, Minami, Sagamihara, Kanagawa 252-0374, Japan

[3]Department of Stem Cell Research, Fukushima Medical University, 1 Hikarigaoka, Fukushima City, Fukushima 960-1295, Japan

*Author for correspondence (akutsu-h@ncchd.go.jp)

KEY WORDS: *Xist*, Imprinted XCI, Chromatin condensation, Oogenesis, Histone methylation, Nuclear transfer

ABSTRACT

Repression of maternal *Xist* (Xm-*Xist*) during preimplantation in mouse embryos is essential for establishing imprinted X chromosome inactivation. Nuclear transplantation (NT) studies using nuclei derived from non-growing (ng) and full-grown (fg) oocytes have indicated that maternal-specific repressive modifications are imposed on Xm-*Xist* during oogenesis, as well as on autosomal imprinted genes. Recent studies have revealed that histone H3 lysine 9 trimethylation (H3K9me3) enrichments on Xm-*Xist* promoter regions were involved in silencing at the preimplantation stages. However, whether H3K9me3 is imposed on Xm-*Xist* during oogenesis is not known. Here, we dissected the chromatin states in ng and fg oocytes and early preimplantation-stage embryos. Chromatin immunoprecipitation experiments against H3K9me3 revealed that there was no significant enrichment within the Xm-*Xist* region during oogenesis. However, NT embryos with ng nuclei (ngNT) showed extensive Xm-*Xist* derepression and H3K9me3 hypomethylation of the promoter region at the 4-cell stage, which corresponds to the onset of paternal *Xist* expression. We also found that the chromatin state at the *Xist* genomic locus became markedly condensed as oocyte growth proceeded. Although the condensed Xm-*Xist* genomic locus relaxed during early preimplantation phases, the extent of the relaxation across Xm-*Xist* loci derived from normally developed oocytes was significantly smaller than those of paternal-*Xist* and ngNT-*Xist* genomic loci. Furthermore, Xm-*Xist* from 2-cell metaphase nuclei became derepressed following NT. We propose that chromatin condensation is associated with imprinted *Xist* repression and that skipping of the condensation step by NT leads to *Xist* activation during the early preimplantation phase.

INTRODUCTION

Expression of the large non-coding RNA 'X-inactive specific transcript' (*Xist*) is essential for the initiation of X chromosome inactivation (XCI) in female mice and humans[1-3]. In mice, *Xist* expression is initiated around the 4-cell stage and is restricted to the paternal allele[1,2,4]. This expression pattern leads to the establishment of imprinted XCI in extra-embryonic tissues[5]. Paternal Xist (Xp-*Xist*) expression is driven by the deposition of maternal Rnf12/RLIM[6,7]. However, the *Xist* locus on the maternal X chromosome (Xm) is tightly protected by epigenetic factors. Using parthenogenetic embryos, which are composed of 2 maternal genomes, we previously demonstrated that histone 3 lysine 9 trimethylation (H3K9me3) is essential for Xm-*Xist* repression during early preimplantation phases[8].

Using a nuclear transplantation (NT) technique, bi-maternal embryos were constructed from non-growing (ng) and fully grown (fg) oocytes[9]. XCI in the extra-embryonic tissues of bi-maternal embryos predominantly occurred on the allele from ng oocytes[10]. The results indicated that the *Xist* loci of ng oocytes are in specifically permissive states for activation and that Xm-*Xist* imprints are established during oogenesis, as are those of autosomal imprinted genes. However, Xm-*Xist* silencing was observed in primordial germ cells[11], suggesting that *in vivo*, repressive modifications were already imposed on the Xm-*Xist* prior to oogenesis. In addition, *Xist* dysregulation commonly occurred in cloned mouse embryos from various cell types such as somatic and embryonic stem cells[12,13]. Considering that NT is an artificial system, it does not exclude the possibility that NT embryos might not be faithfully reprogrammed. Therefore, in the present study we scrutinized the regulation of Xm-*Xist* by H3K9me3 and chromatin state in NT embryos derived from ng oocytes (ngNT).

RESULTS AND DISCUSSION

H3K9me3 is comparable between ng and fg oocytes at Xm-*Xist* loci

We initially confirmed that Rnf12 is highly expressed during oogenesis (Fig. S1), as described elsewhere[6], indicating that the *Xist* repressive state is established prior to oocyte maturation. We previously demonstrated that H3K9me3 is essential for Xm-*Xist* repression in preimplantation embryos[8]. To examine the chromatin states at *Xist* loci, we used an advanced system of embryo chromatin immunoprecipitation combined with TaqMan gene expression (eChIP-qPCR), which facilitated chromatin analysis of many loci from small numbers of cells. We targeted 19 regions in the *Xist* genes containing promoter regions and a *Gapdh* promoter region as a negative control region for H3K9me3 modification. Our eChIP-qPCR system robustly correlated with the conventional method (no preamplification) (1.21–1.57-fold increase in eChIP-qPCR; correlation between the 2 methods was >0.96, Fig. S2). We therefore examined H3K9me3 in ng and fg oocytes. eChIP-qPCR in ng oocytes revealed that the H3K9me3 levels of the 19 *Xist* regions examined were markedly higher than that of the *Gapdh* promoter region (Fig. 1); specifically, the levels in the *Xist* promoter regions were 6-fold higher. The repressive states across the entire *Xist* region were maintained in fg oocytes, and there were no significant differences between ng and fg oocytes in H3K9me3 levels at any of the *Xist* regions analysed (Fig. 1). These results indicated that transcriptional repressive states were imposed by H3K9me3 in ng oocytes and that the modifications were not established during oogenesis.

Specific loss of H3K9me3 at Xm-*Xist* promoter regions following NT

Our findings showed that the *in vivo* repressive histone H3K9me3 modifications were already imposed on Xm-*Xist* prior to the initiation of oogenesis. Generally, immunofluorescence (IF) analysis showed that after fertilization, global H3K9me3 was specifically imposed on the maternal genome[14,15]. Interestingly, the lack of H3K9me3 was not restricted to the sperm genome. IF analysis revealed that global H3K9me3 levels at the 1-cell stage were markedly lower in the genomes from somatic and embryonic stem (ES) cells compared with maternal genomes[16] (Fig. S3a). However, the dramatically low H3K9me3 levels in ES cell and sperm genomes were not observed at the 2- and 4-cell stages (Fig. S3b). These observations implied that the relaxed chromatin state characterized by low H3K9me3 levels at the 1-cell stage might be important for subsequent *Xist* expression in early preimplantation phases.

To ascertain chromatin states, we constructed NT embryos with ng oocyte genomes (ngNT) and performed IF analysis against H3K9me3. We first examined whether the Xm-*Xist* of ngNT was derepressed at the 4-cell stage. Fluorescence *in situ* hybridization (FISH) analysis for *Xist* RNA showed extensive *Xist* expression (Fig. 2a), confirming that derepression of Xm-*Xist* in ngNT commenced at early preimplantation phases. Next, we conducted IF analysis for H3K9me3 at the 1-cell stage in ngNT constructed by serial NT [17]. Unexpectedly, compared with control embryos (fgNT), there were no apparent reductions in H3K9me3 modifications in ngNT, and the same modifications were observed at the 1-cell to 4-cell stage (Fig. 2b). The signals of H3K9me3 in ngNT and fgNT were significantly higher than those of fertilized embryos (parental genomes) (Fig. 2b), consistent with a previous report that Ring1b—but not H3K9me3—is enriched in paternal constitutive heterochromatin[18].

We also examined the expression states of H3K9me3-associated genes[19-22] (erasers: *Kdm4a/b/c*, writers: *Suv39h1/2*, *Setdb1*) at the 4-cell stage of ngNT and found that the expression levels varied among the ngNT, as well as between control group embryos (Fig. S3c). Although only *Kdm4a* was markedly reduced in most ngNT, it did not seem to affect H3K9me3. These results indicated that global ng genomic H3K9me3 following NT was comparable to that of the fg oocyte genome.

However, a previous study has shown Xm-*Xist* activation to be accompanied by promoter demethylation[8]. Thus, we then asked whether Xm-*Xist* derepression of ngNT embryos at the 4-cell stage could be attributed to the loss of H3K9me3 at *Xist* promoter regions. To reduce the number of embryos required for eChIP-qPCR analysis, we constructed tetraploid ngNT by repressing second polar body release. The tetraploid ngNT also showed Xm-*Xist* derepression at the 4-cell stage (Fig. S4). As expected, H3K9me3 modifications at *Xist* major promoter regions in tetraploid ngNTs at the 4-cell stage declined dramatically (less than 15% of the control) (Fig. 2c). The A repeat regions showed slight demethylation (around 60% of control), consistent with previous results of H3K9me3 demethylase-mediated Xm-*Xist* derepression[8]. Thus, intrinsic Xm-*Xist* protection by H3K9me3 was not maintained following NT.

Genome-wide loss of H3K9me2 in ngNT embryos at the 1-cell stage

We further examined H3K9me2 and H3K27me3 in ngNT embryos because both were shown to be specifically imposed on maternal genomes in zygotes[8,14,23]. H3K27me3 levels of ng and fg oocyte genomes were comparable (Fig. S5a). However, H3K9me2 signals in ngNT were much lower than those in fgNT (Fig. S5a), although low levels of global H3K9me2 were only observed at the 1-cell stage, with no apparent

differences at the 2- and 4-cell stages (Fig. S5b). Although the loss of H3K9me2 in the maternal genome did not affect Xm-*Xist* derepression[8], given that H3K9me2 is inversely related to gene expression at a genome-wide scale[24], the genome-wide lack of H3K9me2 at the 1-cell stage suggested that the chromatin of ng oocytes might be loosened following NT.

Chromatin condensation of *Xist* genomic loci during oogenesis and relaxation in early preimplantation

Consistent with the above notion, DNA methylation levels were shown to dramatically change during oogenesis, and high levels of DNA methylation were observed only in fg oocyte genomes[25]. We were tempted to speculate that maternal genomes might become transcriptionally silent via chromatin condensation. To test this, we carried out DNA-FISH experiments using probes spanning XqD, which contains *Xist*, and measured the distance between loci (Fig. 3a). Many studies have normalized distance with this method by calculating the nuclear radius visualized by 4′,6-diamidino-2-phenylindole (DAPI) staining[26-28]. However, the chromatin in fg oocytes surrounds the nucleolus, and the DAPI-positive area does not totally cover the regions enclosed by the nuclear membrane[29]. Therefore, to determine accurate nuclear radii in fg oocytes, we conducted IF against histone deacetyltransferase 2 (HDAC2), which occurs specifically in the nuclear area. Furthermore, a report has shown the predominant expression of HDAC2 in fg oocytes during oogenesis (Fig. S6a)[30]. The distance in the fg oocyte genome was therefore normalized by the average radius, whereas the distance of the ng oocyte genome was normalized by the DAPI-positive nuclear area (average of ng oocyte examined). DNA-FISH analysis showed that the

genomic regions containing *Xist* were significantly condensed in fg oocytes even without normalization (Fig. 3b and S6b), indicating that the chromatin of the *Xist* genomic locus became condensed during oogenesis.

Next, we conducted DNA-FISH experiments at the 2- and 4-cell stages in ngNT, parthenogenetic (derived from fg oocytes), and androgenetic embryos (containing *Xist* genomic loci derived from paternal X chromosomes). At the 2-cell stage, the distance between loci in ngNT embryos was significantly larger or smaller than that of parthenogenetic, fgNT or androgenetic embryos, respectively (Fig. 3c). However, at the 4-cell stage, the distance was comparable to that of androgenetic embryos but significantly larger than that of parthenogenetic and fgNT embryos (Fig. 3d). Thus, the open chromatin state in ng oocytes was maintained following NT, suggesting that chromatin condensation is likely essential for *Xist* repression.

Imprinted Xm-*Xist* silencing in early embryonic cells is not reprogrammed following NT

We also found that the distance become larger following cell division (Fig. 3b–d), implying that chromatin becomes gradually relaxed during the early cleavage stage, probably reflecting zygotic gene activation. Thus, we suggested that although 4-cell stage parthenogenetic embryo Xm-*Xist* was silenced, the chromatin might be looser than in fg oocytes and thus might be derepressed following NT. We therefore produced 2-cell parthenogenotes arrested at the metaphase by Nocodazol treatment and conducted NT experiments[31] (Fig. 4a). *Xist* RNA-FISH revealed that Xm-*Xist* of NT embryos derived from arrested nuclei of 2-cell parthenogenotes (wherein imprinted *Xist* silencing was maintained) was robustly expressed at the 4-cell stage (Fig. 4b: 77% of nuclei).

These results indicated that imprinted *Xist* repression associated with open chromatin states in donor cells was not faithfully reprogrammed following NT.

Conclusions

As imprinted *Xist* expression is not common in other species, the observed genome condensation during oogenesis might specifically occur on the murine X chromosome. Accordingly, we found that X-linked gene expression levels in mice markedly declined during oogenesis, whereas they were only slightly reduced in mature human oocytes[32].

The NT studies in mice showed *Xist* upregulation regardless of donor cell origins[13], even if the *Xist* imprint was maintained in donor cells such as from early preimplantation embryos (Fig. 4b). Furthermore, considering that H3K9me3 demethylases and histone acetyltransferases are expressed in oocytes[8,33], the Xm-*Xist* promoter in ngNT could be subjected to demethylation owing to chromatin decondensation (Fig. 4c). Overall, our results suggest—as previously proposed by Sado and Sakaguchi[2]—that chromatin condensation is associated with imprinted *Xist* repression on the maternal X at the early preimplantation stage, and that skipping of the condensation step by NT leads to precocious activation of *Xist* activation in during early preimplantation embryos.

MATERIALS AND METHODS

Animals

All mice were maintained and used in accordance with the Guidelines for the Care and Use of Laboratory Animals of the Japanese Association for Laboratory Animal Science and the National Research Institute for Child Health and Development of Japan (A2006-009-C09).

Fluorescence *in situ* hybridization (FISH)

RNA-FISH analysis was performed according to a previous report[8]. In brief, an *Xist* probe (provided by T. Sado) was prepared using a Nick Translation Kit (Abbott Laboratories) and Cy3-dUTP (GE Healthcare Life Sciences).

For DNA-FISH, BAC clones (RP23-311P7: *Xist*/*Tsix* regions and RP23-36C20: *Slc16a2/Rnf12* regions) were purchased from Life Technologies. DNA probes of RP23-311P7 and RP23-36C20 were prepared using the Nick Translation Kit with Cy5-dUTP and Cy3-dUTP, respectively. The procedures were as previously reported. In brief, fixation (2% paraformaldehyde) and permeabilisation (0.25% Triton X-100) were simultaneously conducted for 5 min at room temperature, and then the samples were plated onto glass slides. After RNaseA treatment, the samples were incubated in 0.2N HCl containing 0.5% Triton X-100 on ice for 10 min. The images were obtained by LSM510 laser scanning confocal microscopy using a Plan-Apochromat 100×/1,46 Oil DIC objective (Carl Zeiss).

Distance measurements were based on previous reports[26-28]. Briefly, the signal centroid was calculated by NIH ImageJ software (http://rsb.info.nih.gov/ij/). Each

nuclear radius except for those of fg oocytes used for distance normalization was calculated using the DAPI-stained area measurement.

The full methods were shown in Supplementary information.

Acknowledgements

We are grateful to Dr. T. Sado for the initial proposal of the genomic condensation study, critical reading of the manuscript, and helpful comments. We also thank T. Takigashira and T. Kawasaki for microscopic observation studies and preparation of the Figures, respectively.

Competing interests

The authors declare no competing or financial interests.

Author contributions

A.F. and H.A. conceived the idea. A.F. designed the experiments. A.F. and A.M. conducted all experiments and data analysis. A.U. T. M. and H.A. generated materials and provided analytic tools. H.A. supervised the study. A.F. and H.A. wrote the manuscript.

Funding

This work was supported by grants from the Ministry of Education, Culture, Sports, Science, and Technology (MEXT) of Japan; a grant from the Ministry of Health, Labor, and Welfare (MHLW) to H.A. and A.U.; a Grant-in-Aid for Scientific Research (21390456); a grant from JST-CREST to H.A.; and a JSPS KAKENHI Grant-in-Aid for Young Scientists (B) to A.F. (26861350).

Figures

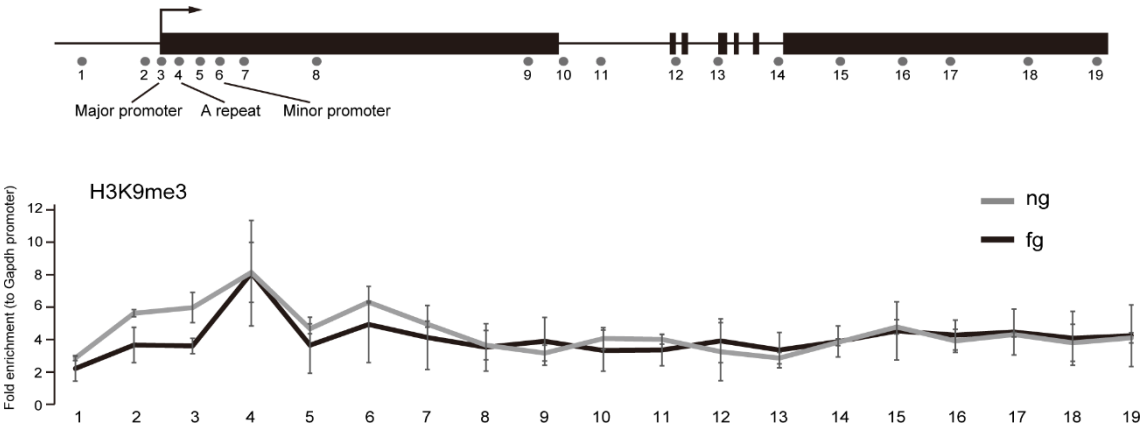

Fig. 1. H3K9me3 states in ng and fg oocytes by eChIP-qPCR analysis.

A total of 19 regions in *Xist* were analysed by eChIP-qPCR. Positions 3, 4, and 6 were localized in the major promoter, A repeat, and minor promoter, respectively. There were no significant differences among the regions tested. Three independent experiments were carried out, and the error bars show the standard error of the mean (s.e.m).

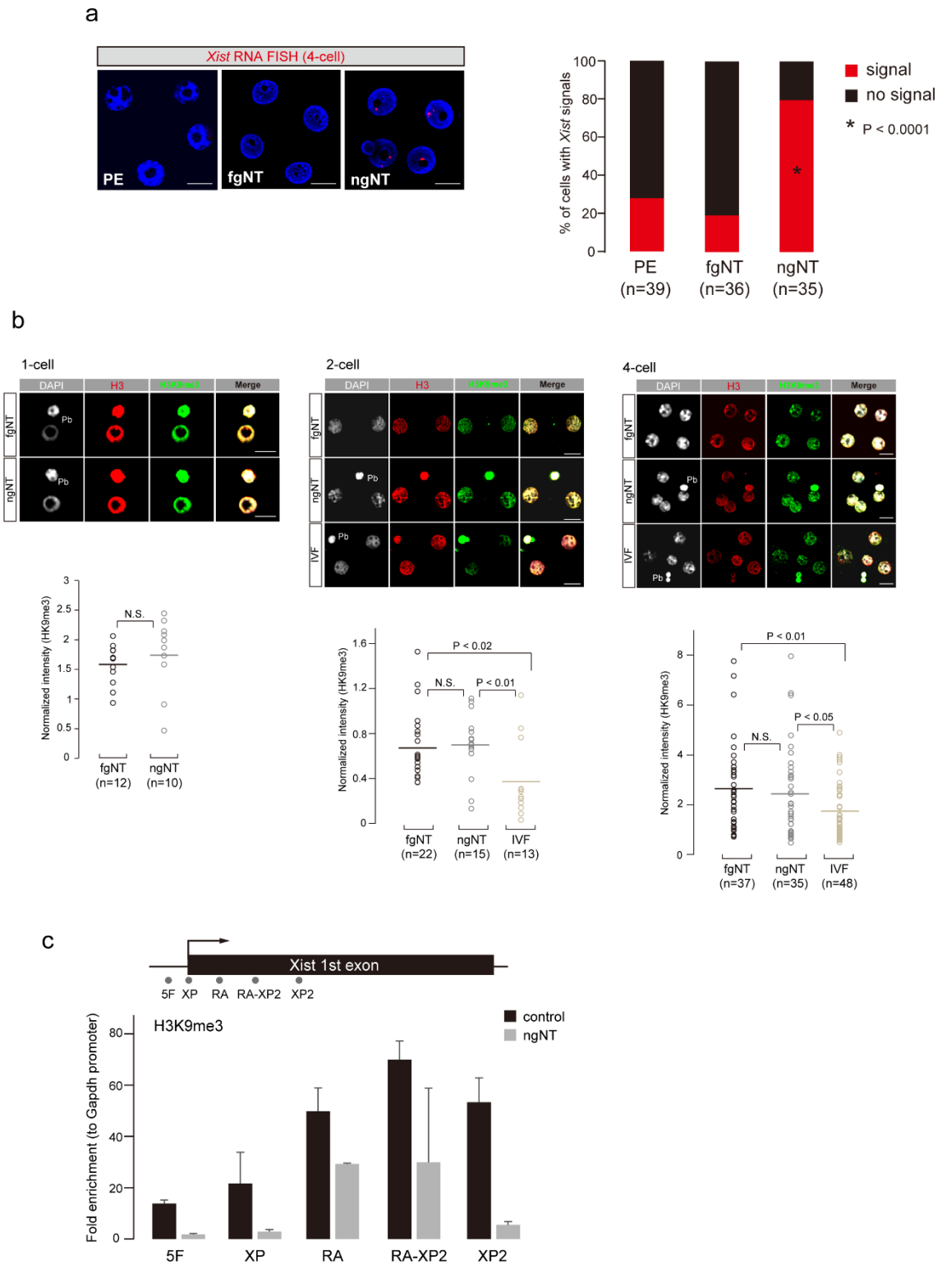

Fig. 2. Loss of H3K9me3 in ngNT embryos at Xm-*Xist* promoter regions but not genome wide. (a) *Xist* RNA-FISH analysis at the 4-cell stage of ngNT (diploid ng genomes), fgNT (diploid fg genomes), and parthenogenetic (diploid fg genomes) embryos. Nuclei stained with 4′ ,6-diamidino-2-phenylindole (DAPI) are shown in blue. *Xist* is shown in red. n represents the number of analysed nuclei. The P-values were calculated using Fisher's exact test (compared to PE and fgNT, respectively). (b) IF analysis of H3K9me3 in ngNT embryos and control (fgNT) embryos constructed by serial NT at the 1-cell stage. fgNT and ngNT embryos were produced by single NT at 2- and 4-cell stages. For comparison with fertilized embryos, *in vitro* fertilized (IVF) embryos were prepared. n represents the number of analysed nuclei. The scale bar represents 20 μm. DAPI, H3, and H3K9me3 are shown in white, red, and green, respectively. The H3K9me3 signal intensity was normalized by the H3 signal. n represents the number of analysed nuclei. The P-values were calculated using Student's t-test. (c) eChIP-qPCR analysis of ngNT and control (tetraploid fgNT) embryos at the 4-cell stage. H3K9me3 at Xm-*Xist* promoter regions of tetraploid embryos in both groups were analysed by eChIP-qPCR. Two independent experiments were conducted, and error bars show s.e.m.

a

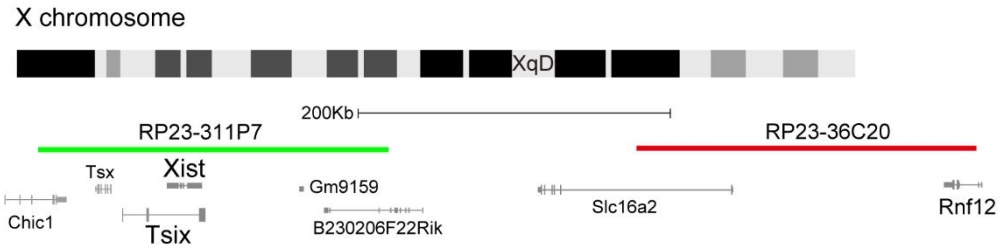

b

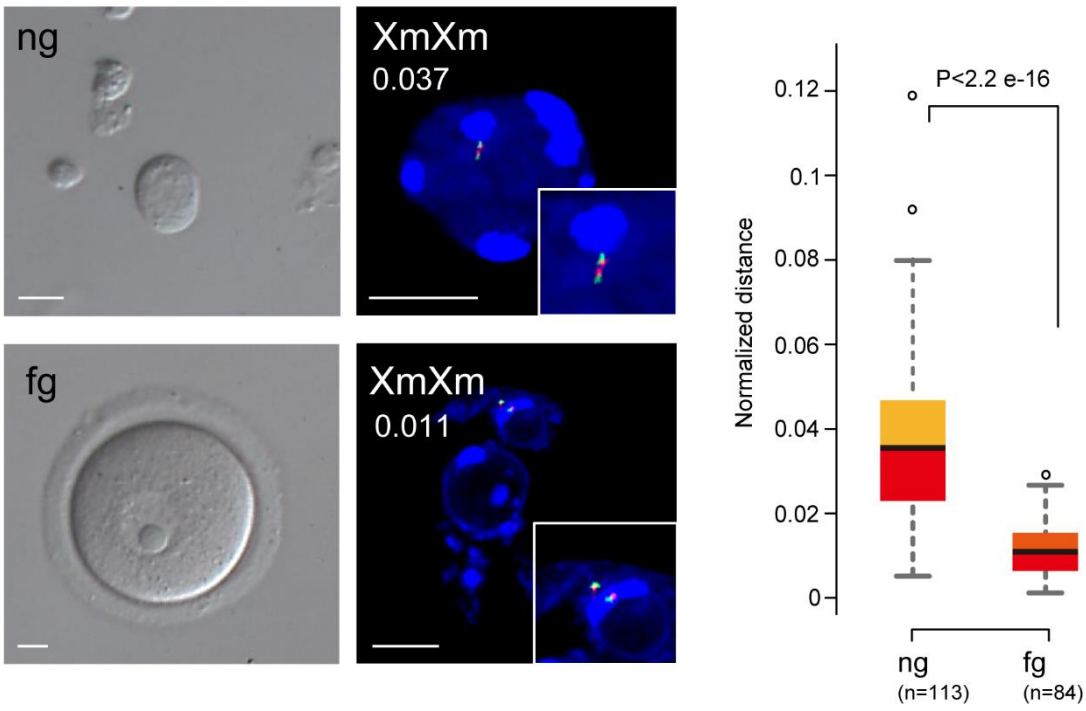

c

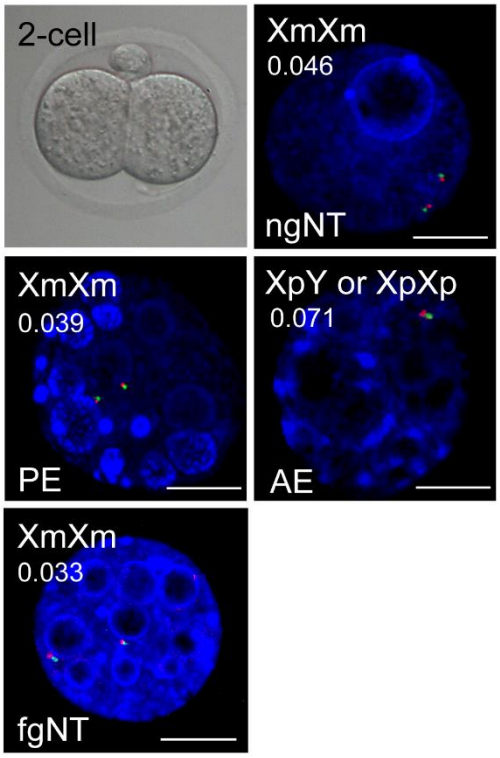
2-cell
XmXm
0.046
ngNT
XmXm
0.039
PE
XpY or XpXp
0.071
AE
XmXm
0.033
fgNT

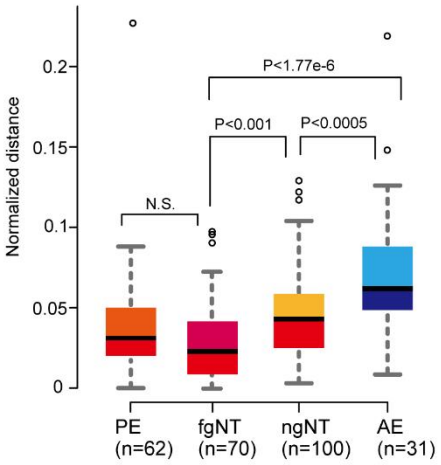
Normalized distance
0.2
0.15
0.1
0.05
0
P<1.77e-6
P<0.001
P<0.0005
N.S.
PE
(n=62)
fgNT
(n=70)
ngNT
(n=100)
AE
(n=31)

d

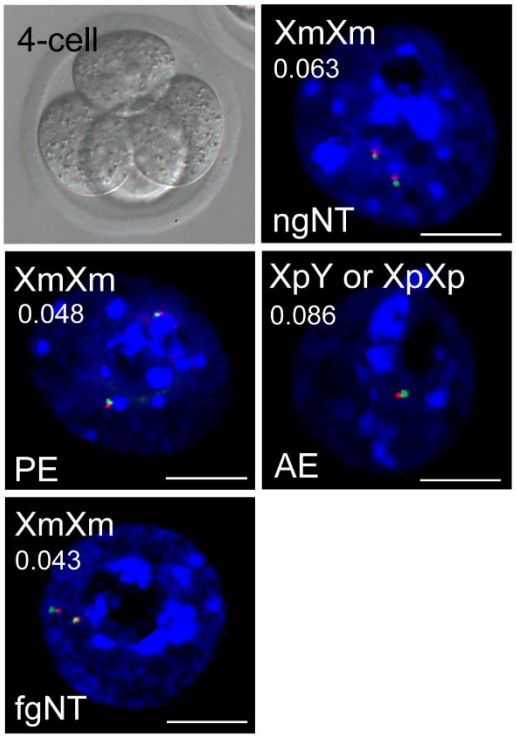
4-cell
XmXm
0.063
ngNT
XmXm
0.048
PE
XpY or XpXp
0.086
AE
XmXm
0.043
fgNT

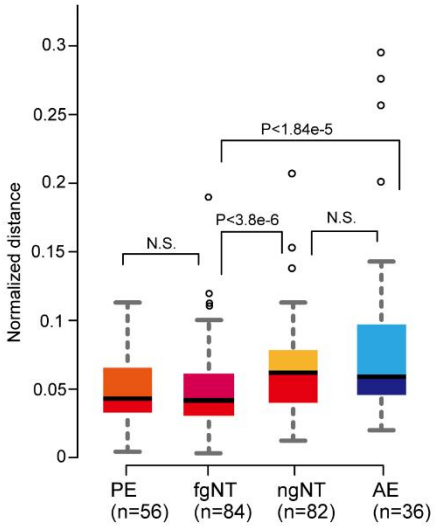
Normalized distance
0.3
0.25
0.2
0.15
0.1
0.05
0
P<1.84e-5
P<3.8e-6
N.S.
N.S.
PE
(n=56)
fgNT
(n=84)
ngNT
(n=82)
AE
(n=36)

Fig. 3. DNA FISH analysis at the *Xist* genomic loci in ng and fg oocytes and various preimplantation embryos. (a) The measurement of the distance between centroids of each signal by DNA-FISH using BAC clones. The BAC clone colours correspond with the signals below the analysis. (b–d) DNA-FISH analysis in ng and fg oocytes and (b) in parthenogenetic (PE: diploid fg genomes), fgNT (diploid fg genome), ngNT (diploid ng genomes), and androgenetic (AE: diploid sperm genomes) embryos at 2- (c) and 4-cell (d) stages. n represents the number of analysed signals. The boxplot indicates the normalized distances, and P-values were calculated by Mann–Whitney U tests. Xm and Xp represent the maternal and paternal X chromosomes, respectively. The scale bar shows 10 μm. Nuclei stained with DAPI are shown in blue. Average values of normalized distance are shown in each picture.

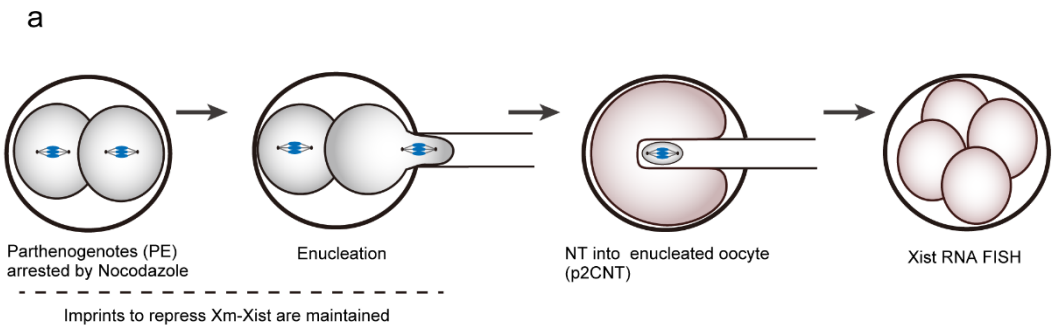

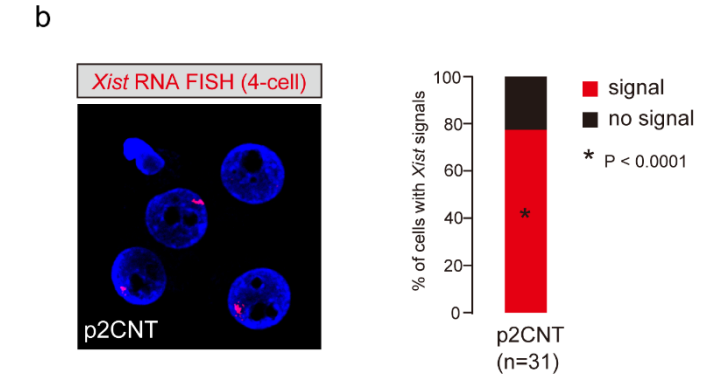

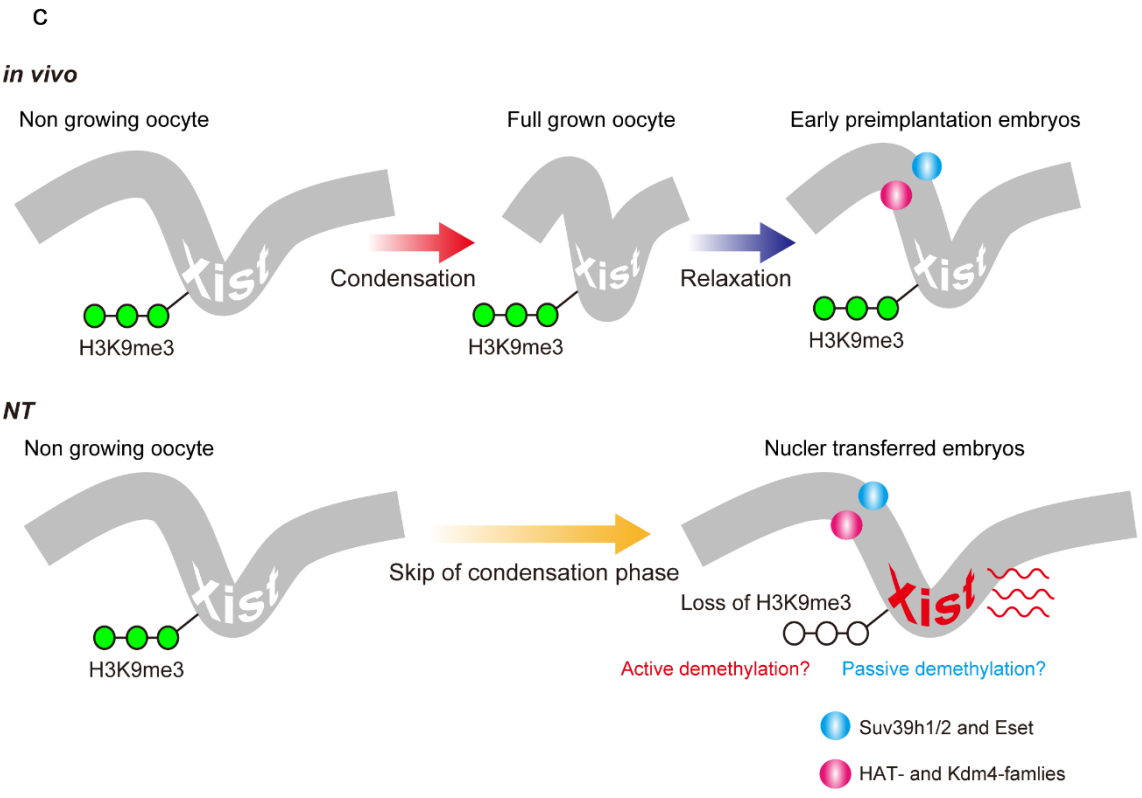

Fig. 4. Imprinted Xm-*Xist* silencing in early embryonic nuclei are not reprogrammed following NT. (a) Experimental scheme of embryonic NT. Diploid parthenogenetic 2-cell embryos were incubated in the presence of Nocodazol (0.1 μg/mL) for 12 h and washed in M2 medium to form spindles. Condensed nuclei of metaphase-arrested 2-cell parthenogenotes (PE) were transferred into enucleated oocytes (p2CNTs). (b) *Xist* RNA-FISH analysis of p2CNT embryos at the 4-cell stage. The bar graph shows the *Xist* expression states in each embryo. P-values were calculated by Fisher's exact tests in comparison with the PE and fgNT embryos in Fig. 2a. (c) Model of Xm-*Xist* silencing machinery from oogenesis to early preimplantation phases. During oogenesis, Xm-*Xist* loci are condensed, but become relaxed in early preimplantation phases. NT skips the condensation phase to result in Xm-*Xist*, which is in a permissive state for activation. During oocyte and early preimplantation stages, some H3K9me3 demethylases and histone acetylases are expressed[8,33]. Open chromatin might cause active or passive demethylation.

References

1. Augui, S., Nora, E.P. & Heard, E. Regulation of X-chromosome inactivation by the X-inactivation centre. *Nat Rev Genet* **12**, 429-42 (2011).
2. Sado, T. & Sakaguchi, T. Species-specific differences in X chromosome inactivation in mammals. *Reproduction* **146**, R131-9 (2013).
3. Lee, J.T. Gracefully ageing at 50, X-chromosome inactivation becomes a paradigm for RNA and chromatin control. *Nat Rev Mol Cell Biol* **12**, 815-26 (2011).
4. Nesterova, T.B., Barton, S.C., Surani, M.A. & Brockdorff, N. Loss of Xist imprinting in diploid parthenogenetic preimplantation embryos. *Dev Biol* **235**, 343-50 (2001).
5. Takagi, N. & Sasaki, M. Preferential inactivation of the paternally derived X chromosome in the extraembryonic membranes of the mouse. *Nature* **256**, 640-2 (1975).
6. Shin, J. *et al.* Maternal Rnf12/RLIM is required for imprinted X-chromosome inactivation in mice. *Nature* **467**, 977-81 (2010).
7. Jonkers, I. *et al.* RNF12 is an X-Encoded dose-dependent activator of X chromosome inactivation. *Cell* **139**, 999-1011 (2009).
8. Fukuda, A. *et al.* The role of maternal-specific H3K9me3 modification in establishing imprinted X-chromosome inactivation and embryogenesis in mice. *Nat Commun* **5**, 5464 (2014).
9. Kono, T., Obata, Y., Yoshimzu, T., Nakahara, T. & Carroll, J. Epigenetic modifications during oocyte growth correlates with extended parthenogenetic development in the mouse. *Nat Genet* **13**, 91-4 (1996).
10. Tada, T. *et al.* Imprint switching for non-random X-chromosome inactivation during mouse oocyte growth. *Development* **127**, 3101-5 (2000).
11. Sugimoto, M. & Abe, K. X chromosome reactivation initiates in nascent primordial germ cells in mice. *PLoS Genet* **3**, e116 (2007).
12. Inoue, K. *et al.* Impeding Xist expression from the active X chromosome improves mouse somatic cell nuclear transfer. *Science* **330**, 496-9 (2010).
13. Fukuda, A. *et al.* Identification of inappropriately reprogrammed genes by large-scale transcriptome analysis of individual cloned mouse blastocysts. *PLoS One* **5**, e11274 (2010).
14. Santos, F., Peters, A.H., Otte, A.P., Reik, W. & Dean, W. Dynamic chromatin modifications characterise the first cell cycle in mouse embryos. *Dev Biol* **280**, 225-36 (2005).

15. Kageyama, S. *et al.* Alterations in epigenetic modifications during oocyte growth in mice. *Reproduction* **133**, 85-94 (2007).
16. Wang, F., Kou, Z., Zhang, Y. & Gao, S. Dynamic reprogramming of histone acetylation and methylation in the first cell cycle of cloned mouse embryos. *Biol Reprod* **77**, 1007-16 (2007).
17. Kawahara, M. *et al.* Protocol for the production of viable bimaternal mouse embryos. *Nat Protoc* **3**, 197-209 (2008).
18. Puschendorf, M. *et al.* PRC1 and Suv39h specify parental asymmetry at constitutive heterochromatin in early mouse embryos. *Nat Genet* **40**, 411-20 (2008).
19. Peters, A.H. *et al.* Loss of the Suv39h histone methyltransferases impairs mammalian heterochromatin and genome stability. *Cell* **107**, 323-37 (2001).
20. Matsui, T. *et al.* Proviral silencing in embryonic stem cells requires the histone methyltransferase ESET. *Nature* **464**, 927-31 (2010).
21. Greer, E.L. & Shi, Y. Histone methylation: a dynamic mark in health, disease and inheritance. *Nat Rev Genet* **13**, 343-57 (2012).
22. Klose, R.J. & Zhang, Y. Regulation of histone methylation by demethylimination and demethylation. *Nat Rev Mol Cell Biol* **8**, 307-18 (2007).
23. Nakamura, T. *et al.* PGC7 binds histone H3K9me2 to protect against conversion of 5mC to 5hmC in early embryos. *Nature* **486**, 415-9 (2012).
24. Wen, B., Wu, H., Shinkai, Y., Irizarry, R.A. & Feinberg, A.P. Large histone H3 lysine 9 dimethylated chromatin blocks distinguish differentiated from embryonic stem cells. *Nat Genet* **41**, 246-50 (2009).
25. Shirane, K. *et al.* Mouse oocyte methylomes at base resolution reveal genome-wide accumulation of non-CpG methylation and role of DNA methyltransferases. *PLoS Genet* **9**, e1003439 (2013).
26. Terranova, R. *et al.* Polycomb group proteins Ezh2 and Rnf2 direct genomic contraction and imprinted repression in early mouse embryos. *Dev Cell* **15**, 668-79 (2008).
27. Eskeland, R. *et al.* Ring1B compacts chromatin structure and represses gene expression independent of histone ubiquitination. *Mol Cell* **38**, 452-64 (2010).
28. Chambeyron, S. & Bickmore, W.A. Chromatin decondensation and nuclear reorganization of the HoxB locus upon induction of transcription. *Genes Dev* **18**, 1119-30 (2004).
29. De La Fuente, R. Chromatin modifications in the germinal vesicle (GV) of mammalian oocytes. *Dev Biol* **292**, 1-12 (2006).
30. Ma, P., Pan, H., Montgomery, R.L., Olson, E.N. & Schultz, R.M. Compensatory

functions of histone deacetylase 1 (HDAC1) and HDAC2 regulate transcription and apoptosis during mouse oocyte development. *Proc Natl Acad Sci U S A* **109**, E481-9 (2012).

31. Egli, D., Sandler, V.M., Shinohara, M.L., Cantor, H. & Eggan, K. Reprogramming after chromosome transfer into mouse blastomeres. *Curr Biol* **19**, 1403-9 (2009).

32. Fukuda, A., Tanino, M., Matoba, R., Umezawa, A. & Akutsu, H. Imbalance between the expression dosages of X-chromosome and autosomal genes in mammalian oocytes. *Sci Rep* **5**, 14101 (2015).

33. Yoshida, N., Brahmajosyula, M., Shoji, S., Amanai, M. & Perry, A.C. Epigenetic discrimination by mouse metaphase II oocytes mediates asymmetric chromatin remodeling independently of meiotic exit. *Dev Biol* **301**, 464-77 (2007).